DOI:10.1021/jf1006853

JOURNAL OF AGRICULTURAL AND FOOD CHEMISTRY
ARTICLE

Production and Properties of Nanocellulose-Reinforced Methylcellulose-Based Biodegradable Films

Ruhul A. Khan,[†,⊥] Stephane Salmieri,[†] Dominic Dussault,[†] Jorge Uribe-Calderon,[§] Musa R. Kamal,[§] Agnes Safrany,[#] and Monique Lacroix*,[†]

[†]Research Laboratory in Sciences Applied to Food, Canadian Irradiation Center (CIC), INRS-Institute Armand-Frappier, University of Quebec, 531 Boulevard des Prairies, Laval, Quebec H7V 1B7, Canada, [§]Department of Chemical Engineering, McGill University, 3610 University Street, Montreal, Quebec H3A 2B2, Canada, [#]Section of Industrial Applications and Chemistry, Department of Physical and Chemical Sciences, Division of Nuclear Sciences and Applications, International Atomic Energy Agency, Vienna International Centre, P.O. Box 100, A-1400 Vienna, Austria A2371, and [⊥]Nuclear and Radiation Chemistry Division, Institute of Nuclear Science and Technology, Bangladesh Atomic Energy Commission, Dhaka 1000, Bangladesh

Methylcellulose (MC)-based films were prepared by casting from its 1% aqueous solution containing 0.5% vegetable oil, 0.25% glycerol, and 0.025% Tween 80. Puncture strength (PS), puncture deformation (PD), viscoelasticity coefficient, and water vapor permeability (WVP) were found to be 147 N/mm, 3.46 mm, 41%, and 6.34 g·mm/m^2·day·kPa, respectively. Aqueous nanocellulose (NC) solution (0.1−1%) was incorporated into the MC-based formulation, and it was found that PS was improved (117%) and WVP was decreased (26%) significantly. Films containing 0.25% NC were found to be the optimum. Then films were exposed to γ radiation (0.5−50 kGy), and it was revealed that mechanical properties of the films were slightly decreased after irradiation, whereas barrier properties were further improved with a decrease of WVP to 28.8% at 50 kGy. Molecular interactions due to incorporation of NC were supported by FTIR spectroscopy. Thermal properties of the NC-containing films were improved, confirmed by TGA and DSC. Crystalline peaks appeared due to NC addition, found by XRD. Micrographs of films containing NC were investigated by SEM.

KEYWORDS: Packaging materials; biodegradable films; methylcellulose; nanocellulose; γ radiation

INTRODUCTION

Petroleum-based synthetic polymers are used as packaging materials due to their excellent thermomechanical properties and also for economical reasons. Unfortunately, these materials are not biodegradable. Thus, efforts are in progress to develop alternative packaging materials that are environmentally friendly, cheap, and lightweight, possess good thermomechanical properties, and provide a good barrier to moisture, gas, and solid transfer. Typical materials under consideration are based on cellulosic-type compound-, lipid-, and protein-based biodegradable materials. Biodegradable films made of these materials do not pose a threat to the environment and are also cost-effective. However, the disadvantages of these films include poor thermomechanical properties and a strongly hydrophilic nature. Therefore, many studies are now attempting to overcome theses drawbacks to approach physicochemical attributes analogous to those of petrochemical polymers (*1*−*5*).

Cellulose is the most abundant organic polymer in the biosphere. It is the main constituent of plants; moreover, it is lightweight, biodegradable, and available as renewable resources. There is a major interest in using cellulosic materials as the main components in the manufacture of biodegradable packaging materials (*6*−*8*). Methylcellulose (MC) is a derivative of cellulose and can be produced from cotton cellulose, wood, and annual plant pulps. It is produced by chemical treatments via alkali-cellulose using concentrated NaOH solution. Alkali-cellulose is then treated with methyl halide (or dimethyl sulfate) to produce MC. MC has been widely used for many years to produce gels and fine chemicals in pharmaceuticals, foods, construction, paints, ceramics, detergents, agriculture, polymerization, adhesives, and cosmetics. According to their physicochemical properties, MCs can be also employed as emulsifiers, medicine constituents, colloidal stabilizers, viscosity controllers, and flow controllers. MC shows good solubility in water at low temperature (*9*−*13*).

Nanocellulose (NC) is also a cellulose derivative composed of a nanosized fiber network, which determines the product properties and its functionality. NC fibers are very interesting nanomaterials for production of cheap, lightweight, and very strong nanocomposites. NC fibers have nanosized diameters (2−20 nm), and lengths ranging from a few hundred nanometers to a few micrometers (*14*). NC is expected to show high stiffness because the Young's modulus of the cellulose crystal is as high as 134 GPa. A considerable amount of research has been done on the isolation of these nanofibers from plants for use as fillers in biocomposites.

*Author to whom correspondence should be addressed [telephone (450) 687-5010; fax (450) 686-5501; e-mail monique.lacroix@iaf.inrs.ca].

 Published on Web 06/15/2010

Cellulose nanofibers are recognized as being more effective than their microsized counterparts to reinforce polymers due to interactions between the nanosized elements that form a percolated network connected by hydrogen bonds, provided there is a good dispersion of the nanofibers in the matrix. It is predicted that NC reinforcements in the polymer matrix may provide value-added materials with superior performance and extensive applications for the next generation of biodegradable materials (*15*−*18*).

The application of γ radiation is becoming more widespread every year. Over the past four decades, there has been a continuous and significant growth in the development and application of radiation techniques, primarily in the coating and adhesive industries. As this technique continues to develop innovative products based on high efficiency and easy process control, a logical extension for this technology is found to be in the field of polymer composites. The use of γ radiation offers several advantages, such as continuous operation, minimum time requirement, less atmospheric pollution, curing at ambient temperatures, and increased design flexibility through process control. When cellulosic materials are subjected to γ radiation, radicals are produced on the cellulose chain by hydrogen and hydroxyl abstraction. γ Radiation also ruptures some carbon−carbon bonds and produces radicals. Chain scission may also take place to form other radicals. γ Radiation produces three types of reactive species in cellulose-based polymers. These are ionic, radical, and peroxide. The peroxide species are produced when polymers are irradiated in the presence of oxygen. The effect of γ radiation on organic polymers produced ionization and excitation; as a resultm some free radicals are produced. γ Radiation can be used for the treatment of foods to preserve quality. The integrity of food products irradiated at high doses (> 10 kGy) is already established (*19*−*22*).

The objective of the present research was to evaluate the effect of incorporation of NC on the thermomechanical properties of MC-based cast biodegradable films. The mechanical properties of the films were measured to evaluate their puncture strength (PS), puncture deformation (PD), and viscoelasticity coefficient (*Y*). Water vapor permeability (WVP) tests were carried out to investigate the moisture barrier properties of films under specified conditions. Molecular interactions of components due to the incorporation of NC in MC-based films were examined by Fourier transform infrared (FTIR) spectroscopy. Thermal properties of the films were investigated by thermogravimetric analysis (TGA) and differential scanning calorimetry (DSC). Crystallinity due to NC addition in MC-based films was analyzed by X-ray diffraction (XRD). Surface morphology was investigated by scanning electron microscopy (SEM). Films were also exposed to γ radiation from the range of low dose (0.5 kGy) to high dose (50 kGy) to determine the effects on the mechanical properties of the films.

MATERIALS AND METHODS

Materials. Methylcellulose (powder form; viscosity of 400 cP for a 1% solution at 20 °C) was purchased from Sigma-Aldrich Canada Ltd. (Oakville, ON, Canada). Nanocellulose was provided generously by FPInnovations Paprican (Pointe-Claire, QC, Canada). Glycerol and Tween 80 were from Laboratoire Mat (Beauport, QC, Canada). Vegetable oil (Sunflower brand) was obtained from a local grocery.

Film Preparation. MC solution (1% w/w) was prepared in an ice bath using deionized water with continuous stirring. Aqueous NC (0.1−1%) solution was prepared at 60 °C and sonicated for 30 min at room temperature. Then 0.5% vegetable oil (hydrophobic agent), 0.25% glycerol (plasticizer), and 0.025% Tween 80 (emulsifier) along with the NC solution (reinforcing agent, i.e., filler) were directly poured into the MC solution. The mixture was then homogenized using an IKA T25 digital Ultra-Turrax disperser (IKA Works Inc., Wilmington, NC) at 45 °C and 24000 rpm for 1 min. Films were then cast by applying 12 mL of the film-forming solution onto Petri dishes (100 mm × 15 mm; VWR International, Ville Mont-Royal, QC, Canada) and allowed to dry for 24 h, at room temperature and 35% relative humidity (RH). Dried water-soluble films were peeled off manually using a spatula and stored in polyethylene bags prior to characterization.

Irradiation. Irradiation of films was conducted with γ-rays generated from a ^{60}Co source at room temperature, at a dose rate of 17.878 kGy/h (0.3578 kGy/min) in an Underwater Calibrator-15A Research Irradiator (MDS Nordion Inc., Kanata, ON, Canada).

Measurement of the Mechanical Properties of MC-Based Films. *Film Thickness*. Film thickness was measured using a Mitutoyo Digimatic Indicator (Type ID-110E; Mitutoyo Manufacturing Co. Ltd., Tokyo, Japan) with a resolution of 0.001 mm, at five random positions around the film, by slowly reducing the micrometer gap until the first indication of contact.

Puncture Strength and Puncture Deformation. PS and PD were measured using a Stevens-LFRA texture analyzer (model TA-1000; Texture Technologies Corp., Scarsdale, NY). Films were fixed between two perforated Plexiglas plates (3.2 cm diameter), and the holder was held tightly with two screws. A cylindrical probe (2 mm diameter; scale, 0−900 g; sensitivity, 2 V) was moved perpendicularly to the film surface at a constant speed (1 mm/s) until it passed through the film. Strength values at the puncture point were used to calculate the hardness of the film. The PS values were divided by the thickness of the films to avoid any variation related to this parameter. PS was calculated using the equation PS (N/mm) = $(9.81F)/x$, where F is the recorded force value (g), x is the film thickness (μm), and 9.81 $m \cdot s^{-2}$ is the gravitational acceleration. PD of the films was calculated from the PS curve, using the distance (mm) recorded between the time of first probe/film contact and the time of puncture point.

Viscoelasticity (*Y*). Viscoelastic properties were evaluated using relaxation curves. The same puncture test procedure described above was used, but the probe was stopped to 3 mm after film contact and maintained for 1 min. The relaxation coefficient Y was calculated using the equation $Y(\%) = [(F_i - F_f)/F_i] \times 100$, where F_i is the initial recorded value (g) and F_f the second value measured after 1 min of relaxation. A low relaxation coefficient ($Y \rightarrow 0\%$) indicates high film elasticity, whereas a high coefficient ($Y \rightarrow 100\%$) indicates high film plasticity related to a more rigid and easily distorted material.

Water Vapor Permeability. WVP tests were conducted gravimetrically using an ASTM procedure (*23*). Films were mechanically sealed onto Vapometer cells (No. 68-1, Twhing-Albert Instrument Co., West Berlin, NJ) containing 30 g of anhydrous calcium chloride (0% RH). The cells were initially weighed and placed in a Shellab 9010 L controlled humidity chamber (Sheldon Manufacturing Inc., Cornelius, OR) maintained at 25 °C and 60% RH for 24 h. The amount of water vapor transferred through the film and absorbed by the desiccant was determined from the weight gain of the cell. The assemblies were weighed initially and after 24 h for all samples and up to a maximum of 10% gain. Changes in weight of the cell were recorded to the nearest 10^{-4} g. WVP was calculated according to the combined Fick and Henry laws for gas diffusion through coatings and films, according to the equation

$$\text{WVP}\ (g \cdot mm/m^2 \cdot day \cdot kPa) = \Delta w x / A \Delta P$$

where Δw is the weight gain of the cell (g) after 24 h, x is the film thickness (mm), A is the area of exposed film (31.67×10^{-4} m^2), and ΔP is the differential vapor pressure of water through the film (ΔP = 3.282 kPa at 25 °C).

Statistical Analysis. For each measurement, three samples in each replicate were tested. Analysis of variance and Duncan's multiple-range tests were used to perform statistical analysis on all results, using PASW Statistics Base 18 software (SPSS Inc., Chicago, IL). Differences between means were considered to be significant when $p \leq 0.05$.

Fourier Transform Infrared Spectroscopy. FTIR spectra of the films were recorded using a Spectrum One spectrophotometer (Perkin-Elmer, Woodbridge, ON, Canada) equipped with an attenuated total reflectance (ATR) device for solids analysis and a high-linearity lithium tantalate (HLLT) detector. Spectra were analyzed using Spectrum 6.3.5 software. Films were stored at room temperature for 72 h in a desiccator

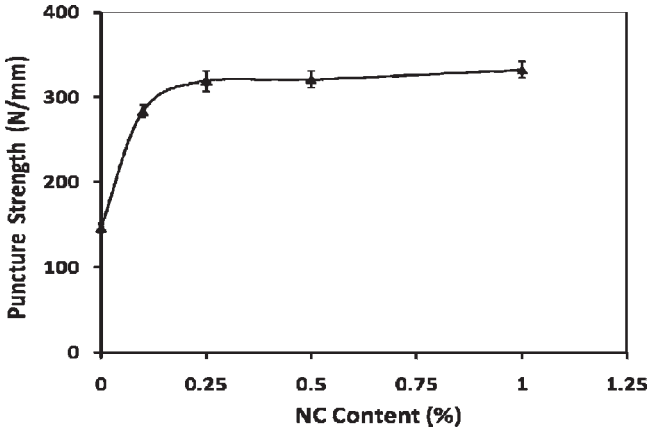

Figure 1. Effect of nanocellulose (NC) content on the puncture strength (PS) of methylcellulose-based films.

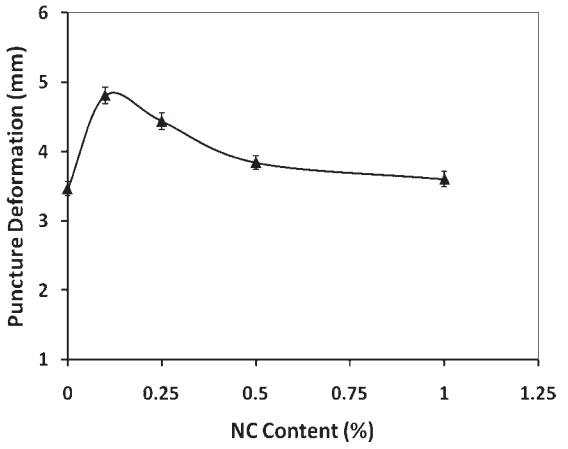

Figure 2. Effect of nanocellulose (NC) content on the puncture deformation (PD) of methylcellulose-based films.

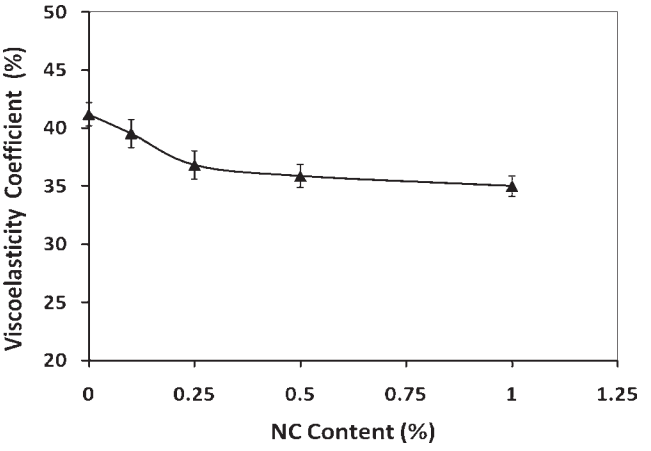

Figure 3. Effect of nanocellulose (NC) content on the viscoelasticity coefficient (Y) of methylcellulose-based films.

containing saturated NaBr solution to ensure a stabilized atmosphere of 59.1% RH at 20 °C. Films were then placed onto a zinc selenide crystal, and the analysis was performed within the spectral region of 650−4000 cm^{-1} with 64 scans recorded at a 4 cm^{-1} resolution. After attenuation of total reflectance and baseline correction, spectra were normalized with a limit ordinate of 1.5 absorbance units. The resulting FTIR spectra were compared to evaluate the effects of NC filling in the MC films, based on the intensity and shift of vibrational bands.

Thermogravimetric Analysis . TGA of the films was carried out using a TGA 7 (Perkin-Elmer) analyzer. The experiment was carried out under an argon atmosphere (40 cm^3/min). The weight of the film samples varied from 5 to 10 mg, and the scanning range was maintained to 50−600 °C.

Differential Scanning Calorimetric Analysis. DSC analysis was carried out using a Pyris DSC calorimeter (Perkin-Elmer). The scanning temperature was from 50 to 200 °C. The scanning process comprised an initial heating followed by cooling, and finally a second temperature scanning was performed. The heating/cooling rate was 10 °C/min, under a nitrogen atmosphere.

X-ray Diffraction. For XRD analysis, film samples were folded several times to increase the sample thickness. Samples were analyzed between $2\theta = 5°$ and 114° with step size $2\theta = 0.02°$ in a D8 Discover X-ray Diffractometer (Bruker AXS Inc., Madison, MI) using a Co Kα (40 kV/35 mA).

Scanning Electron Microscopy Analysis. Film samples (5 × 5 mm) were deposited on an aluminum holder and sputtered with gold−platinum (coating thickness, 150−180 Å) in a Hummer IV sputter coater. SEM photographs were taken with a Hitachi S-4700 FEG-SEM scanning electron microscope (Hitachi Canada Ltd., Mississauga, ON, Canada) at a magnification of 40000×, at room temperature. The working distance was maintained between 15.4 and 16.4 mm, and the acceleration voltage used was 5 kV, with the electron beam directed to the surface at a 90° angle and a secondary electron imaging (SEI) detector.

RESULTS AND DISCUSSION

Mechanical Properties of MC-Based films: Effect of NC Filling. *Puncture Strength*. The PS of MC-based films (thickness ∼ 24 μm) was found to be 146.6 N/mm. To improve mechanical properties and reduce WVP, NC fibers were incorporated, from a 0.1−1% NC aqueous solution, into the MC-based film-forming solution. **Figure 1** shows the effect of NC content on the PS of MC-based films. Incorporation of NC caused a significant increase of PS ($p \leq 0.05$). With 0.1% NC, the PS of the films increased by almost 94%. On the other hand, 0.25, 0.5, and 1% NC contents raised the PS of films by 117, 119, and 126%, respectively. PS values seemed to reach a plateau after 0.25% NC content in MC-based films. Thus, the NC nanofibers acted as a reinforcing agent in MC-based films. NC is composed of crystalline nanofibers (*18*), which impart higher PS values to the MC-based films. Similar observations were reported by Azeredo et al. (*24*). They mentioned that the mechanical properties, except elongation, were improved significantly by the addition of cellulose nanofibers to mango puree edible films. Lee et al. (*25*) observed that the tensile and thermal properties of poly(vinyl alcohol)-based composite films were significantly improved with an increase of NC loading.

Puncture Deformation. The PD value of the MC-based films was found to be 3.5 mm. **Figure 2** shows the effect of NC content on the PD of MC-based films. The incorporation of NC caused a significant rise of PD ($p \leq 0.05$). The largest deformation was 39% higher than control, which was observed for 0.1% NC concentration. Above 0.1% NC concentration, all other films (0.25, 0.5, and 1% NC content) exhibited a continuous decrease of PD values. However, all of the NC-containing specimens showed higher values of PD than the control sample. At higher levels of NC, which acts as a reinforcing filler, the material tends to become somewhat more brittle. This is a common observation in nanocomposites as well as conventional composite materials. Here, NC is acting as a reinforcing agent in MC-based films, so higher amounts of NC can make the films stiffer. The decreased PD values may be related to the increased stiffness of the films by the addition of NC (*26*).

Viscoelasticity Coefficient. **Figure 3** shows the effect of NC content on the viscoelasticity coefficient (Y) of the MC-based films. A two-step gradient discontinued decrease of Y was observed with an increase of NC concentration, including an

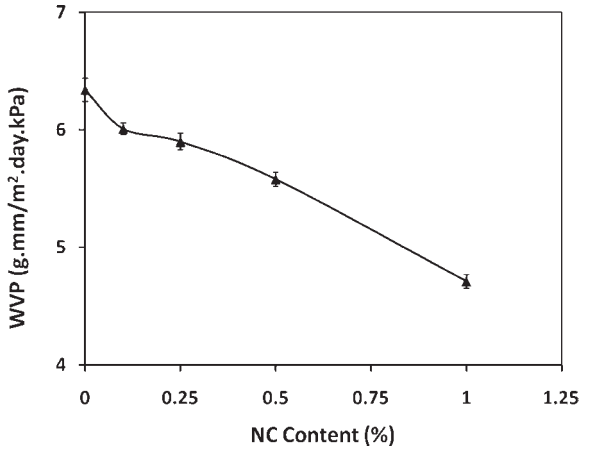

Figure 4. Effect of nanocellulose (NC) content on the water vapor permeability (WVP) of methylcellulose-based films.

inflection point at 0.25% NC and leading to a plateau effect. Thus, a solid-like behavior of films seemed to become more prominent with the increase of NC content, from incorporating 0.25% NC particularly because no significant difference ($p > 0.05$) could be observed in viscoelasticity measurements. The Y coefficient decreased following NC concentrations higher than 0.25%, implying a diminishing contribution of NC to mechanical reinforcement after a saturation concentration of about 0.25%. This result supports the above observations noted for **Figures 1** and **2**. The Y coefficient of MC-based films (without NC) was found to be 41.2% as compared to 39.5, 36.8, 35.9, and 35.0% that were observed for 0.1, 0.25, 0.5, and 1% NC incorporation, respectively. Other researchers also reported decreased relaxation coefficients with the addition of cellulose nanofibers in films (*27*, *28*), hence leading to more viscoelastic films.

Water Vapor Permeability. Figure 4 shows the effect of NC content on the WVP of the MC-based films. The values of WVP decreased sharply as the content of NC in the films increased. Indeed, the WVP of control films (without NC) was 6.3 g·mm/m^2·day·kPa. On the other hand, WVP values were 6.0, 5.9, 5.6, and 4.7 g·mm/m^2·day·kPa for films containing 0.1, 0.25, 0.5, and 1% NC, respectively. Thus, a 26% reduction of WVP was obtained at 1% NC in MC films. The presence of crystalline fibers in NC is thought to increase the tortuosity in the MC-based films, leading to slower diffusion processes and, hence, to a lower permeability (*24*). The barrier properties are enhanced if the filler is less permeable and has a good dispersion into the matrix (*29*). In the present study, the interactions of NC with MC-based films components (mainly cellulose) as well as the interactions between nanofibers may have enhanced the water vapor barrier (*15*). Azeredo et al. (*24*) reported that the WVP of chitosan films was improved significantly by the addition of cellulose nanofibers. They mentioned that a nanocomposite film with 15% cellulose nanofibers and plasticized with 18% glycerol was comparable to synthetic polymers in terms of strength and stiffness.

Effect of γ Radiation. MC-based films were exposed to γ radiation (^{60}Co source) from 0.5 to 50 kGy doses and PS, PD, Y coefficient, and WVP values of the films were measured. The results are presented in **Table 1**. The results show that up to a 10 kGy dose, no significant changes ($p > 0.05$) were observed. However, from 25 kGy, PS and Y coefficient were lowered along with WVP, whereas PD was not different significantly ($p > 0.05$). At a 50 kGy dose, films lost 15% PS, 9% viscoelasticity, and 9% WVP, whereas no significant difference was observed for PD ($p > 0.05$). It seems that irradiation treatment caused a significant decrease ($p \leq 0.05$) of the mechanical properties of MC-based films.

Table 1. Effect of γ Radiation on the Mechanical Properties of MC-Based Films Prepared by Casting[a]

dose (kGy)	PS (N/mm)	PD (mm)	Y (%)	WVP (g·mm/m^2·day·kPa)
0	146 ± 6 c	3.5 ± 0.2 ab	41.2 ± 2.0 d	6.3 ± 0.2 bc
0.5	144 ± 9 c	3.4 ± 0.2 a	40.2 ± 1.2 cd	6.6 ± 0.3 d
1	145 ± 10 c	3.5 ± 0.1 ab	41.0 ± 1.8 d	6.3 ± 0.2 cd
5	146 ± 4 c	3.6 ± 0.1 bc	38.9 ± 2.2 c	6.3 ± 0.1 bc
10	140 ± 12 bc	3.6 ± 0.1 bc	35.4 ± 1.1 b	6.0 ± 0.3 ab
25	132 ± 3 ab	3.6 ± 0.1 bc	33.4 ± 0.6 a	5.9 ± 0.1 a
50	124 ± 5 a	3.7 ± 0.1 c	32.2 ± 1.2 a	5.8 ± 0.2 a

[a] Means followed by the same letter in each column are not significantly different at the 5% level.

Table 2. Effect of γ Radiation on the Mechanical Properties of (MC+0.25% NC)-Based Films Prepared by Casting[a]

dose (kGy)	PS (N/mm)	PD (mm)	Y (%)	WVP (g·mm/m^2·day·kPa)
0	319 ± 16 cd	4.4 ± 0.3 abc	36.8 ± 0.9 b	5.9 ± 0.2 d
0.5	346 ± 15 e	4.4 ± 0.2 bc	36.2 ± 1.2 b	5.9 ± 0.1 d
1	338 ± 12 de	4.5 ± 0.2 c	33.1 ± 0.2 a	5.9 ± 0.3 d
5	318 ± 19 cd	4.4 ± 0.1 abc	33.1 ± 0.8 a	5.3 ± 0.2 c
10	309 ± 22 c	4.3 ± 0.2 abc	33.1 ± 1.2 a	5.0 ± 0.1 b
25	286 ± 15 b	4.2 ± 0.2 a	33.1 ± 0.5 a	4.8 ± 0.2 b
50	256 ± 23a	4.2 ± 0.2 ab	33.0 ± 1.0 a	4.2 ± 0.2 a

[a] Means followed by the same letter in each column are not significantly different at the 5% level.

Indeed, irradiation treatment may have affected the internal structure of cellulose and thus reduced the mechanical properties of films but improved their barrier properties significantly ($p \leq 0.05$). In this context, it could be hypothesized that the action of γ irradiation induced a molecular weight decrease leading to a loss in film strength as well as improved barrier properties due to hydrogen bonding involvement from additional chain ends and rearrangements. Similar results were also reported by Le Tien et al. (*4*) and mentioned that the WVP of whey protein-based films was improved due to γ irradiation treatment.

The MC-based films containing 0.25% NC were also exposed to the same γ irradiation doses from 0.5 to 50 kGy, and mechanical properties were also measured to evaluate the influence of NC incorporation combined with irradiation. Results are presented in **Table 2**. As mentioned earlier, the 0.25% NC concentration was found to be optimal, because films with NC content above 0.25% provided significantly higher PS values ($p \leq 0.05$), but not drastically when compared to the control (see **Figure 1**). **Table 2** shows that, at low doses (0.5−1 kGy), the PS of the films was raised slightly, whereas it started decreasing at higher doses (5−50 kGy). Hypothetically, these results may be due to the presence of NC fibers reoriented unidirectionally along the axis in the MC matrix, in a minute contribution as reinforcing agents. Moreover, from 25 kGy, a significant reduction of PS was observed ($p \leq 0.05$), with 19.7% of PS reduction measured for 50 kGy exposure.

Otherwise, the values of Y coefficient and WVP of the films also decreased significantly ($p \leq 0.05$) with increasing irradiation dose up to 50 kGy (from 1 kGy for Y coefficient and from 5 kGy for WVP), whereas no significant difference was observed for PD ($p > 0.05$). Indeed, a 3.8% loss of Y coefficient and a 28.8% decrease of WVP were measured for (MC+0.25%NC)-based films irradiated at 50 kGy, as compared to control.

FTIR Analysis of the Films. Figure 5 shows the FTIR spectra of (**a**) MC-based films (control), (**b**) MC-based films containing 0.25% NC, (**c**) MC-based films containing 0.5% NC, and (**d**) MC-based films containing 1% NC. Hence, this analysis

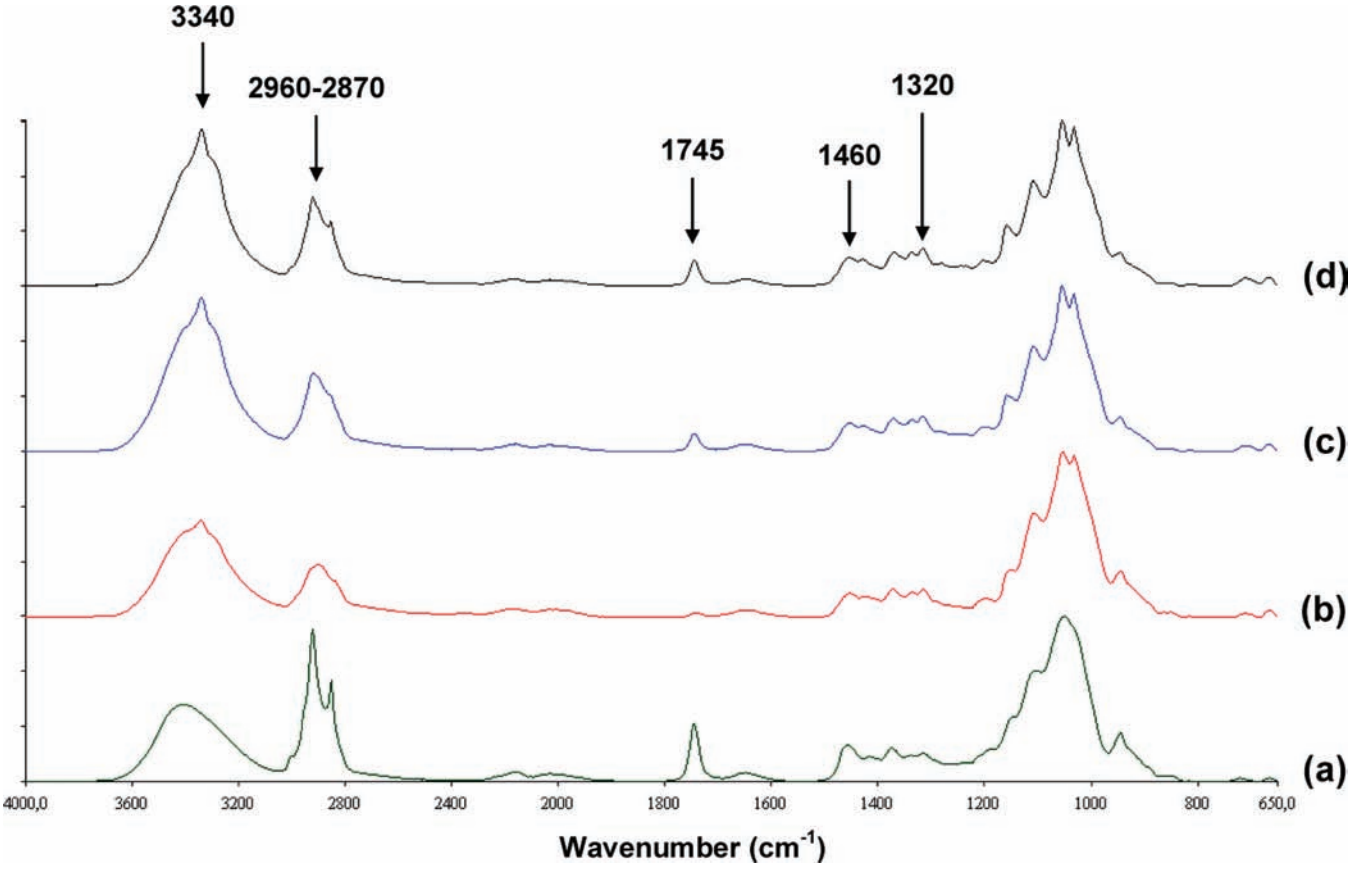

Figure 5. FTIR spectra of MC- (**a**) and (MC+NC)-based films containing 0.25% (**b**), 0.5% (**c**), and 1% NC (**d**) respectively.

attempted to characterize the incorporation of NC into the MC-based film matrix and distinguish the IR bands and vibrations shifts related to NC interactions. The absorption peaks of the MC film spectrum (**a**) are mainly assignable to the stretching vibrations of O−H at 3200−3600 cm^{-1}, overlapping symmetric and asymmetric C−H at 2870−2960 cm^{-1}, and bound water vibration at 1600−1800 cm^{-1}.

Some differences can be observed in the whole IR region after addition of NC into film matrix. Indeed, a strong absorption band can be observed at 3340 cm^{-1} after NC addition for all concentrations, related to the typical O−H vibration of crystalline NC (*30*). In addition to an increased intensity of the O−H band, the presence of hydrogen-bound O−H groups caused a shift of absorption to lower frequencies (down from 3410 to 3330 cm^{-1}), with the appearance of a broadened and asymmetrical peak, as previously reported by Turhan et al. (*31*) and Velasquez et al. (*32*). Otherwise, the intensity of the overall O−H band (3200−3600 cm^{-1}) increases with the NC concentration, suggesting an increase of hydrogen bonding between MC and NC (*16*). It is interesting to note that the ratio O−H elongation/C−H elongation increased significantly with the NC concentration, suggesting an increase of hydrogen bonding as compared to hydrophobic interactions related to methyl groups from MC, as reported by Filho et al. (*33*).

The band at 1745 cm^{-1} corresponds to the bending vibration of O−H from water molecules contained in the film. A significant decrease in intensity of this peak was observed after NC incorporation, suggesting a decrease of bound water in the film. It should be emphasized that this IR region of water resonance has little effect on the interpretation of spectra, as previously reported (*32*). As a result, these interactions related to an increased hydrogen bonding and a decreased level of bound water, as described above, could explain the improvement of barrier properties after NC addition, as illustrated in **Figure 4**.

The region from 1270 to 1500 cm^{-1} corresponds to the typical vibration modes of MC associated with vibrations relating to the degree of order that is observed for typical cellulosic materials, as described by Velasquez et al. (*32*) and Filho et al. (*33*). It was already reported that cellulose and MC had very similar profiles in this region. However, the presence of NC altered the intensity of some peaks. Indeed, as NC concentration increased, a decrease of intensity was observed at 1460 cm^{-1} and an increase of intensity was noted at 1320 cm^{-1}, respectively. A lower intensity at 1460 cm^{-1} could be attributed to a reduced resonance of methylated residues from MC after NC addition (asymmetric bending vibration of $-CH_3$). The higher intensity at 1320 cm^{-1} could be attributed to a more crystalline pattern in the conformation of the oxymethyl groups (bending vibration of $O-CH_2$) from cellulose induced by NC addition, as indicated by Ivanova et al. (*34*) and Usmanov et al. (*35*).

Other bands at 1160, 1110, 1055, 1030, and 950 cm^{-1} have their intensity increased after NC addition. These bands are attributed to typical cellulosic compounds and are assigned to C−O, C−C, and ring structures, in addition to external deformational vibrations of CH_2, C−OH, C−CO, and C−CH groups, as already described (*34*).

Overall, the FTIR spectra of MC-based films containing different concentrations of NC provided insight into the effect of NC concentration on the intensity of IR vibrations related to MC and NC and on the band shift due to modified hydrogen bonding. The secondary structure of the film-forming cellulosic material also seemed to be affected due to the crystalline conformation of NC. With regard to the effect of γ irradiation on the films, no variation in FTIR spectra could be observed clearly

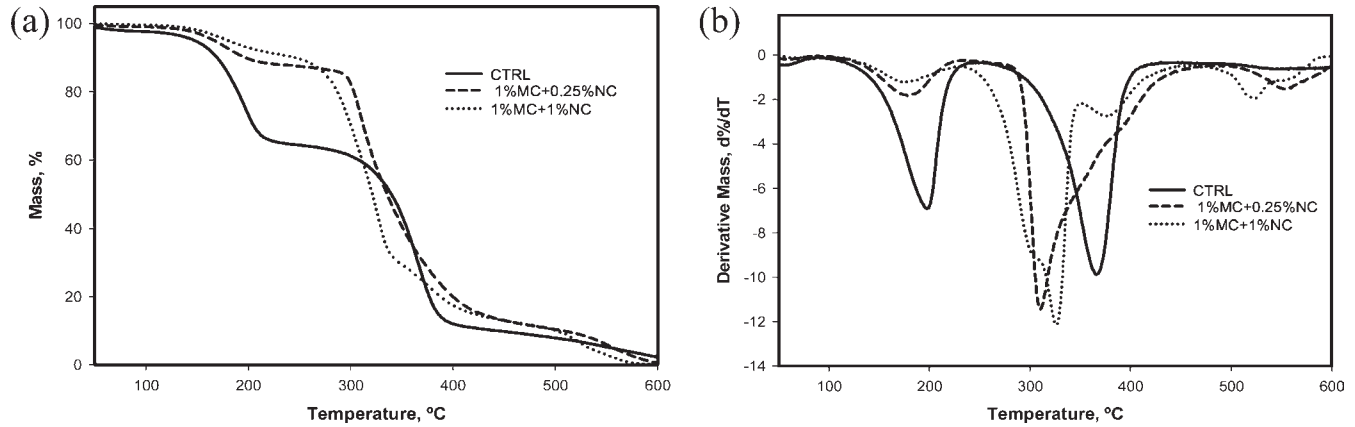

Figure 6. (**a**) TGA and (**b**) derivative TGA curves for MC- and (MC+NC)-based films.

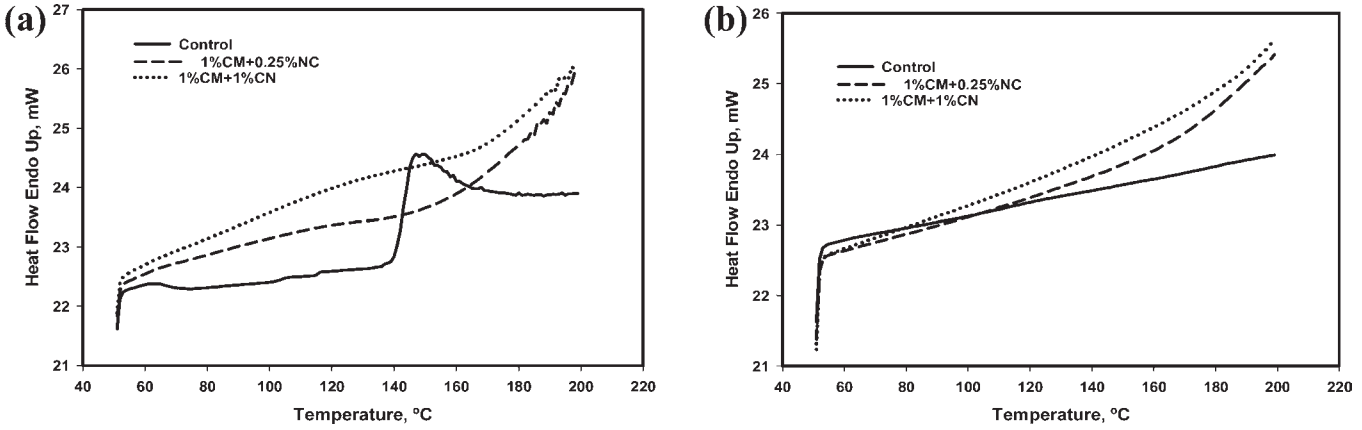

Figure 7. DSC curves for MC- and (MC+NC)-based films: (**a**) first heating cycle; (**b**) second heating cycle.

(spectra not shown). Nevertheless, the spectra were consistent as related to the chemical nature of films, implying analogous vibration bands.

It is noted here that irradiation effect was not investigated on the thermal and morphological properties of films because irradiation decreased the PS of films. Consequently, it was decided not to extend further the study of irradiation effect but to focus on the effect of NC filling on the properties of films, in particular to determine the relationship between NC composition and changes that occur in the internal structure of films.

TGA of the Films: Effect of NC Filling. TGA and derivative TGA curves for different films are shown in **Figure 6**. The control sample (MC-based) exhibited two major degradation steps (**Figure 6a**), a maximum decomposition occurred around 200 and 370 °C for the initial and second decomposition processes, respectively. The first decomposition process can be attributed to the vegetable oil, whereas the second event could be related to the thermal decomposition of glycerol and MC. Samples containing NC (both 0.25 and 1% NC content) showed a significant slowing in thermal decomposition of vegetable oil at 200 °C, which indicated a better thermal stability compared to the control sample. With the increase of NC content from 0.25 to 1% in MC-based films, the thermal decomposition at 200 °C was reduced slightly but was slightly higher at 300 °C, which could be attributed the rapid degradation of NC compared to MC. Derivative curves (**Figure 6b**) also indicated similar effects of thermal stability of the films. Derivative curve intensity depends on the overall composition of samples. Therefore, TGA curves show clearly that addition of NC in MC-based films contributed to a substantial improvement in the thermal stability up to 200 °C.

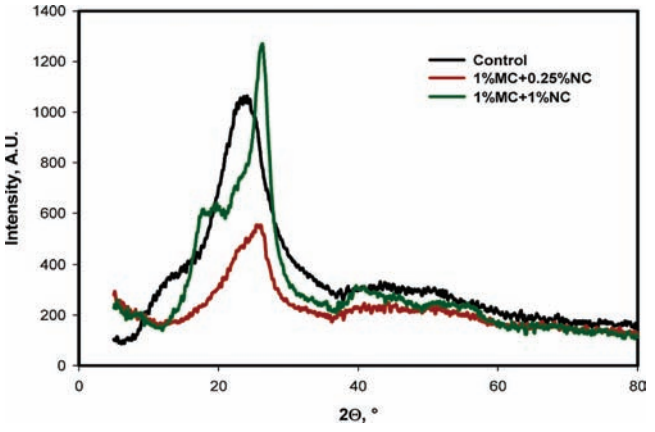

Figure 8. X-ray diffractograms for MC- and (MC+NC)-based films.

DSC Analysis of the Films: Effect of NC Filling. Figure 7a shows the DSC curves for the MC-based films with 0.25 and 1% NC contents. The control sample exhibits a melting peak at around 150 °C, which is associated with the evaporation of vegetable oil used in the formulation. Dramatic results appeared for NC-containing films. Indeed, melting peaks at 150 °C disappeared, which might be attributed to the presence of NC fibers that covered the surface as well as the interface of the MC-based films and thus stabilized the films. Both 0.25 and 1% NC containing films showed similar trends, but the heat flow was increased for higher NC contents in the films. The second DSC cycle is shown in **Figure 7b**, indicating that the curves do not reveal either

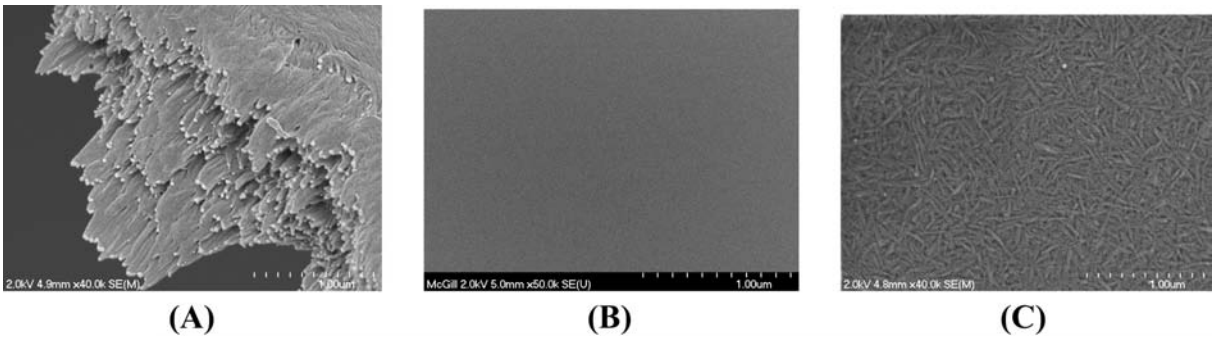

Figure 9. SEM images of (**A**) solid nanocellulose (NC), (**B**) surface of MC-based films (control), and (**C**) surface of (MC+0.25%NC)-based films.

crystalline structures or other transitions. This may be attributable to the thermal degradation/evaporation of some components during the first heating cycle of films.

XRD Analysis: Effect of NC Filling. Figure 8 shows the X-ray diffractograms of MC-based films containing 0.25 and 1% NC. Control films showed a broad halo, which reflected the amorphous nature. Also, films containing lower amounts (0.25%) of NC exhibited similar patterns, but films containing 1% NC showed some crystalline peaks, which may be attributed to the NC fibers in the MC-based formulation. These observations are in accordance with FTIR results, concerning the higher intensity of the crystalline vibrational band of MC at 1320 cm^{-1}, after NC incorporation. Pinitti et al. (*36*) reported the presence of a sharp peak around $2\theta = 8°$ and a broad peak in the region $2\theta = 20.5-21.5°$ for MC films. In this investigation, the control sample (MC-based) showed a broad shoulder in the region around $2\theta = 10-20°$ and a broad peak at $2\theta = 22.9°$. Similar results were reported by Chen et al. (*37*). With an increase of NC concentration in MC-based films (from 0.25 to 1%), the main broad peak shifted to higher angles ($2\theta = 25.5$). At higher NC concentrations, three peaks were observed ($2\theta = 17.2$, 19.0, and 26°). Shin et al. (*38*) supported our results because they indicated that characteristic peaks for crystalline cellulose were in the range of $2\theta = 14.5$, 16.65, and 22.80°. Hence, this investigation suggested that MC-based films with higher NC content exhibited a combination of amorphous and crystalline peaks. This crystallinity along with nanosized fibers in NC-containing films explained the improved mechanical and water barrier properties compared to MC-based films.

SEM Analysis. Figure 9 presents SEM images of solid NC (**A**) and the surfaces of MC-based films without NC (**B**) and MC-based films containing 0.25% NC (**C**). The fracture surface of the solid NC looks like a bundle of fibers presenting a regular and linear sheet-like structure, as observed in **Figure 9A**. This micrograph also indicates a slightly heterogeneous and undulating surface, from which some parts present overlapped small segments close to each other (crystalline structure), whereas other parts present longer segments in a random settlement (amorphous region). The surface of MC-based films (**Figure 6b**) was found to be quite smooth, but surface smoothness was significantly affected after NC incorporation because the NC fibers are clearly visible at the film surface (**Figure 9C**), hence suggesting they are dispersed in a tridimensional network, as expected for a compatible polymer blend. Moreover, the surface of films containing NC appears to be rougher and more condensed, in a separate phase, because they contain a blend of MC and NC, suggesting that NC fibers have kept much of their original physical properties. Overall, the SEM observations seem to support the FTIR structural analysis and provide evidence for the enhanced properties obtained after NC incorporation in film formulation. Similar SEM images of NC fibers were reported by numerous researchers (*18*, *25*, *39*).

In summary, biodegradable MC-based films were successfully prepared by solution casting. Mechanical and water vapor barrier properties of the films were measured. Crystalline NC was added to the film matrix solution before casting to investigate the effect of NC addition on the thermomechanical properties and structure of MC-based films. It was found that NC fibers contributed to the improvement of mechanical and barrier properties in MC-based films. An increase of NC content (0.1−1%) in films allowed increasing the PS and PD of the films significantly ($p \leq 0.05$). WVP of the films containing NC was reduced almost 25% as compared to control, which indicates enhanced moisture barrier properties. FTIR analysis elucidated the molecular interactions involved in NC addition and explained the improvements obtained in properties of films containing NC. Films were exposed to γ radiation (from a low dose of 0.5 kGy to a high dose of 50 kGy), and results revealed that both MC- and (MC+NC)-based films showed significantly lower WVP values ($p \leq 0.05$) at higher doses of radiation, with a minor decrease of PS. From TGA, it was found that NC filling in MC-based films decreased significantly the thermal decomposition of vegetable oil at 200 °C, which indicated a better thermal stability. DSC spectra also supported a better thermal stability of the NC-containing films compared to the control sample, and this is most probably attributed to the NC fibers that are assembled into the film matrix. XRD analysis suggested that NC-containing films gained crystallinity from NC fiber incorporation, due to similar reasons as described for TGA and DSC analysis. SEM analysis of film surface morphology also provided further justification of the improved properties obtained by NC incorporation in films. Moreover, SEM morphological results were in accordance with the molecular interactions changes indicated by FTIR analysis. From all of these corroborating measurements, NC was found to be a satisfactory reinforcing agent in biodegradable cellulosic-based packaging.

ACKNOWLEDGMENT

We thank MDS Nordion for irradiation procedures. We highly appreciate the help of Line Mongeon, Technician of Biomedical Engineering Department and the Facility Electron Microscopy Research FEMR, at the University of McGill for SEM support. We also thank Winpak (Winnipeg, Canada) for providing the packaging material in radiation process.

LITERATURE CITED

(1) Salmieri, S.; Lacroix, M. Physicochemical properties of alginate/polycaprolactone-based films containing essential oils. *J. Agric. Food Chem.* **2006**, *54*, 10205–10214.

(2) Rooney, M. L. Overview of active food packaging. In *Active Food Packaging*; Rooney, M. L., Ed.; Chapman and Hall: London, U.K., 1995; pp 2−36.
(3) Suppakul, P.; Miltz, J.; Sonneveld, K.; Bigger, S. W. Active packaging technologies with an emphasis on antimicrobial packaging and its applications. *J. Food Sci.* **2003**, *68*, 408–420.
(4) Tien, C. L.; Letendre, M.; Ispas-Szabo, P.; Mateescu, M. A.; Delmas-Patterson, G.; Yu, H.-L.; Lacroix, M. Development of biodegradable films from whey proteins by cross-linking and entrapment in cellulose. *J. Agric. Food Chem.* **2000**, *48*, 5566–5575.
(5) Ciesla, K.; Salmieri, S.; Lacroix, M. γ-Irradiation influence on the structure and properties of calcium caseinate-whey protein isolate based films. Part 2. Influence of polysaccharide addition and radiation treatment on the structure and functional properties of the films. *J. Agric. Food Chem.* **2006**, *54*, 8899–8908.
(6) Erdohan, Z. Ö.; Turhan, K. N. Barrier and mechanical properties of methyl cellulose−whey protein films. *Packag. Technol. Sci.* **2005**, *18*, 295–302.
(7) Daiyong, Y.; Farriol, X. Factors influencing molecular weights of methyl celluloses prepared from annual plants and juvenile eucalyptus. *J. Appl. Polym. Sci.* **2006**, *100*, 1785–1793.
(8) Shih, C. M.; Shieh, Y. T.; Twu, Y. K. Preparation and characterization of cellulose/chitosan blend films. *Carbohydr. Polym.* **2009**, *78*, 169–174.
(9) Bain, M. K.; Bhowmik, M.; Ghosh, S. N.; Chattopadhyay, D. *In situ* fast gelling formulation of methyl cellulose for *in vitro* ophthalmic controlled delivery of ketorolac tromethamine. *J. Appl. Polym. Sci.* **2009**, *113*, 1241–1246.
(10) Filho, G. R.; Rosana Assunc, M. N.; Vieira, J. G.; Meireles, C.; Daniel, A.; Cerqueira, D. A.; Barud, H. S.; Ribeiro, S. J. L.; Messaddeq, Y. Characterization of methylcellulose produced from sugar cane bagasse cellulose: crystallinity and thermal properties. *Polym. Degrad. Stab.* **2007**, *92*, 205–210.
(11) Turhan, K. N.; Sahbaz, F.; Güner, A. A spectrophotometric study of hydrogen bonding in methylcellulose-based edible films plasticized by polyethylene glycol. *J. Food Sci.* **2001**, *66* (1), 59–62.
(12) Velazquez, G. A.; Gomez, A. H.; Polo, M. O. Identification of bound water through infrared spectroscopy in methylcellulose. *J. Food Eng.* **2003**, *59*, 79–84.
(13) Bravin, B.; Peressini, D.; Sensidoni, A. Influence of emulsifier type and content on functional properties of polysaccharide lipid-based edible films. *J. Agric. Food Chem.* **2004**, *52*, 6448–6455.
(14) Dieter-Klemm, D.; Schumann, D.; Kramer, F.; Hessler, N.; Koth, D.; Sultanova, B. Nanocellulose materials: different cellulose, different functionality. *Macromol. Symp.* **2009**, *280*, 60–71.
(15) Azeredo, H. M.; Mattoso, L. H.; Avena-Bustillos, R. J. A.; Filho, G. C.; Munford, M. L.; Wood, D.; Mchugh, T. H. Nanocellulose reinforced chitosan composite films as affected by nanofiller loading and plasticizer content. *J. Food Sci.* **2009**, published online.
(16) Cao, X.; Chen, Y.; Chang, P. R.; Muir, A. D.; Falk, G. Starch-based nanocomposites reinforced with flax cellulose nanocrystals. *Polym. Lett.* **2008**, *2* (7), 502–510.
(17) Dongping, S.; Lingli, Z.; Qinghang, W. U.; Shulin, Y. Preliminary research on structure and properties of nano-cellulose. *J. Wuhan Univ. Technol.-Mater. Sci. Ed.* **2007**, 667–680.
(18) Klemm, D.; Schumann, D.; Kramer, F.; Hessler, N.; Hornung, M.; Schmauder, H. P.; Marsch, S. Nanocelluloses as innovative polymers in research and application. *Adv. Polym. Sci.* **2006**, *205*, 49–96.
(19) Khan, M. A.; Khan, R. A.; Zaman, H. U.; Hossain, M. A.; Khan, A. H. Effect of gamma radiation on the physico-mechanical and electrical properties of jute fibre reinforced polypropylene composites. *J. Reinf. Plast. Compos.* **2009**, *28* (13), 1651–1660.
(20) Ghoshal, S.; Khan, M. A.; Noor, F. G.; Khan, R. A. Gamma radiation induced biodegradable shellac films treated by acrylic monomer and ethylene glycol. *J. Macromol. Sci., Part A: Pure Appl. Chem.* **2009**, *46*, 975–982.
(21) Zaman, H. U.; Khan, R. A.; Khan, M. A.; Khan, A. H.; Hossain, M. A. Effect of γ radiation on the performance of jute fabrics reinforced polypropylene composites. *Radiat. Phys. Chem.* **2009**, *78*, 986–993.
(22) Gassan, J.; Bledzki, A. K. The influence of fiber-surface treatment on the mechanical properties of jute−polypropylene composites. *Compos.: Part A* **1997**, *28A*, 1001–1005.
(23) ASTM. *Standard Test Method for Water Vapor Transmission of Materials*; American Society for Testing and Materials: Philadelphia, PA, 1983; Method 15.09:E96.
(24) Azeredo, H. M. C.; Mattoso, L. H. C.; Wood, D.; Williams, T. G.; Bustillos, R. J. A.; McHugh, T. H. Nanocomposite edible films from mango puree reinforced with cellulose nanofibers. *J. Food Sci.* **2009**, *74* (5), 31–35.
(25) Lee, S. Y.; Mohan, D. J.; Kang, I. A.; Doh, G. H.; Lee, S.; Han, S. O. Nanocellulose reinforced PVA composite films: effects of acid treatment and filler loading. *Fibers Polym.* **2009**, *10* (1), 77–82.
(26) Lee, S. Y.; Yang, H. S.; Kim, H. J.; Jeong, C. S.; Lim, B. S.; Lee, J. L. Creep behavior and manufacturing parameters of wood flour filled polypropylene composites. *Compos. Struct.* **2004**, *65*, 459–469.
(27) Samir, M. A. S. A.; Alloin, F; Sanchez, J. Y; Dufresne, A. Cellulose nanocrystals reinforced poly(oxyethylene). *Polymer* **2004**, *45*, 4149–57.
(28) Tang, C.; Liu, H. Cellulose nanofiber reinforced poly(vinyl alcohol) composite film with high visible light transmittance. *Compos.: Part A* **2008**, *39* (10), 1638–1643.
(29) Lagaron, J. M.; Catalá, R.; Gavara, R. Structural characteristics defining high barrier polymeric materials. *Mater. Sci. Technol.* **2004**, *20*, 1–7.
(30) Cao, X.; Dong, H.; Li, C. M. New nanocomposite materials reinforced with flax cellulose nanocrystals in waterborne polyurethane. *Biomacromolecules* **2007**, *8*, 899–904.
(31) Turhan, K. N.; Sahbaz, F.; Güner, A. A spectrophotometric study of hydrogen bonding in methylcellulose-based edible films plasticized by polyethylene glycol. *J. Food Chem.* **2001**, *66*, 59–62.
(32) Velasquez, G.; Herrera-Gómez, A.; Martín-Polo, M. O. Identification of bound water through infrared spectroscopy in methylcellulose. *J. Food Eng.* **2003**, *59*, 79–84.
(33) Filho, G. R.; Assunção, R. M. N.; Vieira, J. G.; Meireles, C. S.; Cerqueira, D. A.; Barud, H. S.; Ribeiro, S. J. L.; Messaddeq, Y. Characterization of methylcellulose produced from sugar cane bagasse cellulose: crystallinity and thermal properties. *Polym. Degrad. Stab.* **2007**, *92*, 205–210.
(34) Ivanova, N. V.; Korolenko, E. A.; Korolik, E. V.; Zhbankov, R. G. IR spectrum of cellulose. *J. Appl. Spectrosc.* **1989**, *51*, 301–306.
(35) Usmanov, K. U.; Yulchibaev, A. A.; Dordzhin, G. S.; Valiev, A. IR spectroscopic analysis of graft co-polymers of cellulose and its derivatives with vinyl fluoride. *Fibre Chem.* **1971**, *3*, 46–48.
(36) Pinottia, A.; Garcia, M. A.; Martinoa, M. N.; Zaritzkya, N. E. Study on microstructure and physical properties of composite films based on chitosan and methylcellulose. *Food Hydrocolloids* **2007**, *21*, 66–72.
(37) Chen, M.; Deng, J.; Yang, F.; Gong, Y.; Zhao, N.; Zhang, X. Study on physical properties and nerve cell affinity of composite films from chitosan and gelatin solutions. *Biomaterials* **2003**, *24*, 2871–2880.
(38) Shin, Y.; Gregory, J.; Exarhos, G. J. Template synthesis of porous titania using cellulose nanocrystals. *Mater. Lett.* **2007**, *61*, 2594–2597.
(39) Auad, M. L.; Contos, V. S.; Nutt, S.; Aranguren, M. I.; Marcovich, N. E. Characterization of nanocellulose reinforced shape memory polyurethanes. *Polym. Int.* **2008**, *57*, 651–659.

Received for review February 18, 2010. Revised manuscript received April 20, 2010. Accepted April 26, 2010. We are grateful to the International Atomic Energy Agency (IAEA) for financial support for a fellowship (IAEA Project Code BGD090/11) and training support offered to R.A.K. and to INRS-Institut Armand-Frappier. This research was supported by the Natural Sciences and Engineering Research Council of Canada (NSERC) through the RDC program and by a research contract under a research agreement with FP Innovation (Pointe-Claire, Canada) and BSA Food Ingredients s.e.c/l.p. The NSERC, le Fond Québécois de la Recherche sur la Nature et les Technologies (FQRNT), and BSA Food Ingredients s.e.c/l.p supported D.D. through the Industrial Innovation Scholarships BMP Innovation.